



Review

Two-dimensional hybrid nanomaterials derived from MXenes ($\text{Ti}_3\text{C}_2\text{T}_x$) as advanced energy storage and conversion applicationsSen Zhao^{a,1}, Ravi Nivetha^{a,1}, Yu Qiu^a, Xiaohui Guo^{a,b,*}^a Key Lab of Synthetic and Natural Functional Molecule Chemistry of Ministry of Education, and the College of Chemistry and Materials Science, Northwest University, Xi'an 710069, China^b The State Key Laboratory of Solidification Processing in Northwestern Polytechnological University, Xi'an 710012, China

ARTICLE INFO

Article history:

Received 17 October 2019

Received in revised form 25 November 2019

Accepted 28 November 2019

Available online 4 December 2019

Keywords:

MXenes

Hybrid nanomaterial

Two-dimensional

Energy storage

Energy conversion

ABSTRACT

The development of two-dimensional hybrid nanomaterial derived from MXenes as high performance electrode material is the key component for the advanced energy storage and conversion systems. In the past decades, MXene derived nanomaterials have attracted greatly interest in scientific activity and potential applications because of their unique synergistic properties such as high thermal stability, excellent electrical conductivity, large surface area, easy to handle and outstanding electro and photo chemical properties. This review is focused on the synthesis of hybrid nanomaterials from MXene ($\text{Ti}_3\text{C}_2\text{T}_x$) for renewable energy conversion and storage application including hydrogen evolution reaction, supercapacitor, lithium-ion batteries and photocatalysis. Finally, we also summarized the prospect and opportunities of novel two-dimensional hybrid nanomaterials derived MXene ($\text{Ti}_3\text{C}_2\text{T}_x$) for futuristic sustainable energy technology

© 2020 Chinese Chemical Society and Institute of Materia Medica, Chinese Academy of Medical Sciences. Published by Elsevier B.V. All rights reserved.

1. Introduction

Rapid growth of population increases the energy demand (17 TW in 2020 to 27 TW by 2040) and causes the increase in associated environmental issues, which urgently inquire us to develop renewable and environmentally friendly solutions to replace fossil fuels [1]. Recent advances in electrochemical energy conversion and storage technologies such as fuel cell, water splitting, supercapacitor and batteries are promising alternative sources for sustainable environment [2]. These advanced electrochemical energy technologies require electrodes with low potential, large active surface area, inexpensive, easy to handle and good conducting materials [3,4]. Noble metals such as Pt, Pd, Au, Ru and their composites are efficient state-of-art electrode material. However, their prohibitive cost and scarcity limit their scalable application [5,6]. To overcome these problems, large efforts have been initiated to improve non-metallic catalysts including transition metal phosphides, metal sulfides and their alloys with higher activity towards energy conversion and storage application.

Although above-mentioned catalysts show good performance, there is still a need to improve their cyclic stability and

performance to replace the noble metal-based catalyst [7]. Therefore, we are yet to identify the wonder catalyst with low cost, high stability and active electrode material, and abundant catalytic active site. Following the advent of two-dimensional material composed of one or two elements such as exfoliation of graphene and other materials like phosphorene, silicene, borophene, germanene, transition -metal dicitenites and oxide [8–13]. It should be noted that, owing to their extraordinary electronic, physical and chemical properties as well as high surface area, optical and mechanical properties, the specific two-dimensional MXenes materials have received highly attentions recently [14–19]. Due to the robust structural stability and excellent electrochemical properties, layered materials with two or more constituent elements offers an excellent opportunity for the myriad of applications [20].

In this regard, a new class of two-dimension transition metal carbides, are referred to as MXenes was discovered by Gogotsi in 2011 [21]. MXene are generally formed from their parent MAX phases, instigated by an expansion of concentrated hydrofluoric acid where etching the Al atom. In most cases, HF was used as a solvent to remove Al layers from the MAX phases to form MXenes [22]. These surfaces functional group provides hydrophilicity nature of MXene that suitable for the aqueous electrolyte system, electrical conductivity and tunable chemistry of Mxene phase [23]. To the best of our knowledge, $\text{Ti}_3\text{C}_2\text{T}_x$ is one of the widely studied MXene phases for energy conversion and storage applications,

* Corresponding author.

E-mail address: guoxh2009@nwu.edu.cn (X. Guo).¹ These authors contributed equally to this work

with well-established etching chemistry [24]. Remarkably, some functional hybrid nanomaterials have been fabricated from MXenes by the partial or complete oxidation process. These hybrids from the oxidation of nanomaterial lead to improved energy conversion and storage performance compared to pristine MXene [25–30]. This review is mainly focused on the synthesis of hybrid nanomaterial from MXene ($\text{Ti}_3\text{C}_2\text{T}_x$) for advanced energy conversion and storage application.

2. Fabrication of 2D hybrid nanomaterial from MXene ($\text{Ti}_3\text{C}_2\text{T}_x$)

Currently, research focuses on the oxidation of Ti_3C_2 into hybrid nanomaterials like TiO_2 and TiN *etc.* For instance, Naguib *et al.* demonstrated the flash oxidation of $\text{Ti}_3\text{C}_2\text{T}_x$ under air atmosphere. $\text{Ti}_3\text{C}_2\text{T}_x$ sample was treated with flash oxidation in air at 1150°C for 30 min. In this synthesis process, it is difficult to control the reaction during the flash oxidation. So, isothermal and hydrothermal oxidization process were explored to prepared TiO_2/C hybrids from $\text{Ti}_3\text{C}_2\text{T}_x$ by the following these steps: (i) $\text{Ti}_3\text{C}_2\text{T}_x$ sample were exposed to the continuous flow of CO_2 (flow rate was 10 sccm) and annealing at required temperature ($150\text{--}500^\circ\text{C}$) for 1 h. Afterwards, the sample was cooled to ambient temperature in an argon atmosphere. (ii) $\text{Ti}_3\text{C}_2\text{T}_x$ sample was dissolved in deionized water and then hydrothermal treatment at required temperature ($150\text{--}250^\circ\text{C}$) with pressure for particular time. After treatment, the final product is obtained *via* washing and further drying treatment. Result shows the conversion of $\text{Ti}_3\text{C}_2\text{T}_x$ into TiO_2 nanocrystals without any structural modification in hydrothermal and flash oxidation conditions, as shown in Fig. 1 [31]. Similar results can be prepared by Guo group, as shown in Fig. 2 [32]. However, due to the strong covalent bond interaction between titanium and carbon atom, no carbon layer exfoliation was observed through this synthesis. Han *et al.* reported the 2D disordered carbon/ TiO_2 composite with a laminated structure was produced *via* annealing of $\text{Ti}_3\text{C}_2\text{T}_x$ nanosheets at 800°C in CO_2 atmosphere (Fig. 3). Through this synthesis, carbon layer is completely exfoliated during the oxidation of $\text{Ti}_3\text{C}_2\text{T}_x$ nanosheets [33]. Recently, Ahmed and coworkers demonstrated the simple and scalable room-temperature oxidation of $\text{Ti}_3\text{C}_2\text{T}_x$ MXene in hydrogen peroxide solution for 5 h. As a result of H_2O_2 treatment, the $\text{TiO}_2/\text{Ti}_2\text{C}$ hybrid material is formed [32]. Further, the above described the as-synthesized layered MXene are bounded together, which maybe hinders the oxidation process [34].

All of these synthesis producers resulted in a slight difference in particle size and morphologies and lead to the formation of carbon supported TiO_2 derived from $\text{Ti}_3\text{C}_2\text{T}_x$. Besides, Guo *et al.* fabricated a novel 2D carbon wrapped TiN hybrids from $\text{Ti}_3\text{C}_2\text{T}_x$ by the

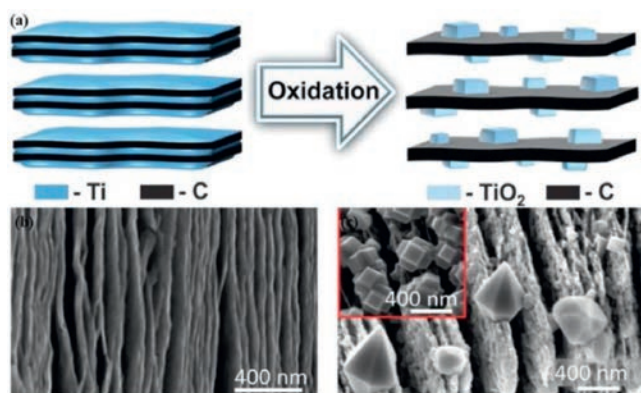


Fig. 1. (a) Schematic illustration the formation of synthesis route of MXene derived TiO_2 nanocrystalline. (b, c) FESEM image of MXene ($\text{Ti}_3\text{C}_2\text{T}_x$) and after oxidation. Reproduced with permission [31]. Copyright 2014, Royal Society of Chemistry.

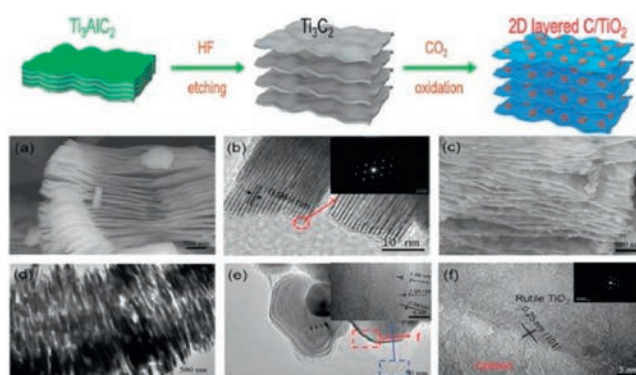


Fig. 2. Schematic represent the formation of 2D layered C/ TiO_2 from MXene ($\text{Ti}_3\text{C}_2\text{T}_x$). (a–f) SEM image of Ti_3C_2 (a), TEM image of Ti_3C_2 (inset: SAED image of Ti_3C_2) (b), SEM image of 2D-layered C/ TiO_2 (c), TEM image of 2D-layered C/ TiO_2 (d), HRTEM image with red color (inset: SAED image of rutile TiO_2) (e, f). Reproduced with permission [32]. Copyright 2017, Wiley Online Library.

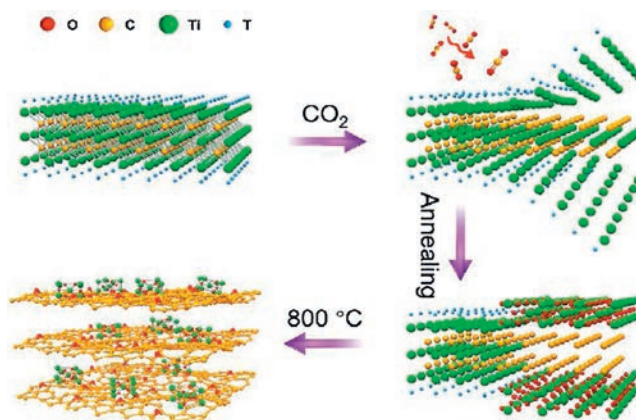


Fig. 3. Schematic of the formation of TiO_2/C hybrids from $\text{Ti}_3\text{C}_2\text{T}_x$ by oxidation process at 800°C in CO_2 environment. T represents the terminating groups consisting of OH, F and O. Reproduced with permission [32]. Copyright 2017, American Chemical Society.

nitridation process at 750°C in NH_3 atmosphere [35]. Wherein, the NH_3 molecules can destroy the titanium–carbon bonds, followed by the formation of Ti-N bond that carbon atom can react with H atom in NH_3 and generate CH_4 molecules which has been decomposed into C and H atoms at elevated temperature. The

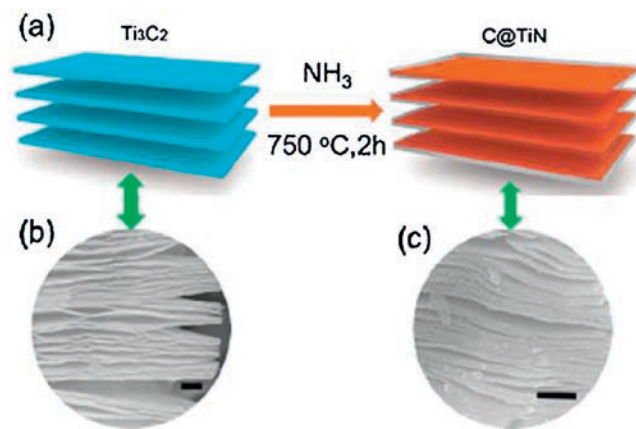


Fig. 4. (a) Schematic represent the formation of C@ TiN from $\text{Ti}_3\text{C}_2\text{T}_x$ MXene. (b, c) FESEM image of Ti_3C_2 and after nitridation. Reproduced with permission [35]. Copyrights 2018, Royal Society of Chemistry.

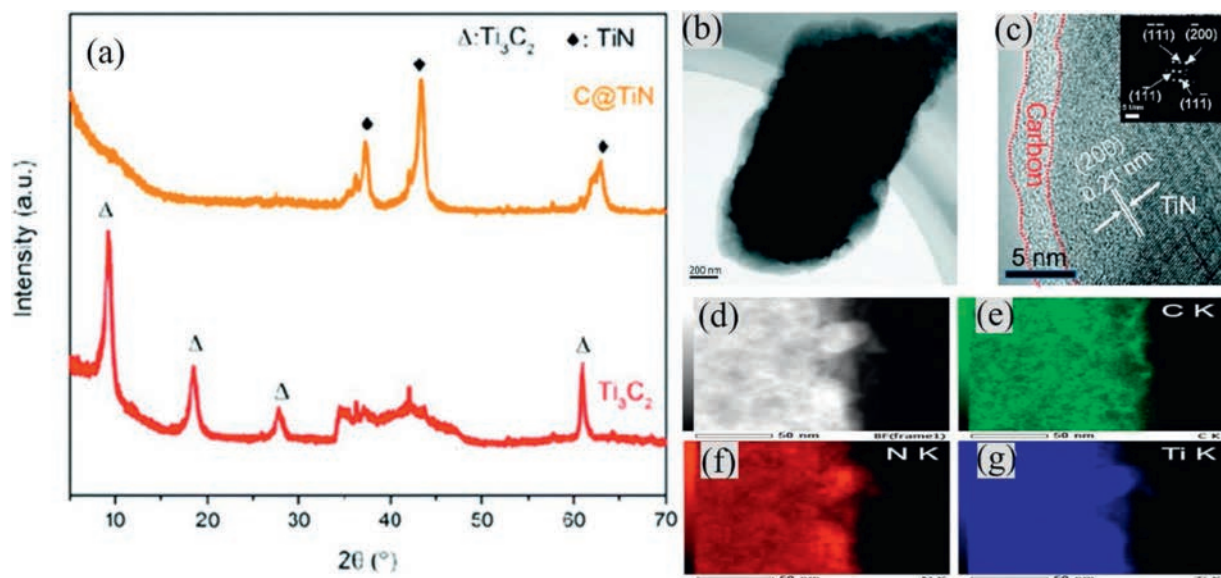


Fig. 5. (a) The XRD pattern of Ti₃C₂ and C@TiN, (b) TEM image of C@TiN, (c) High resolution-TEM image of C@TiN and (d–g) EDX mapping image of C (e) N (f), Ti (g). Reproduced with permission [35]. Copyright 2018, Royal Society of Chemistry.

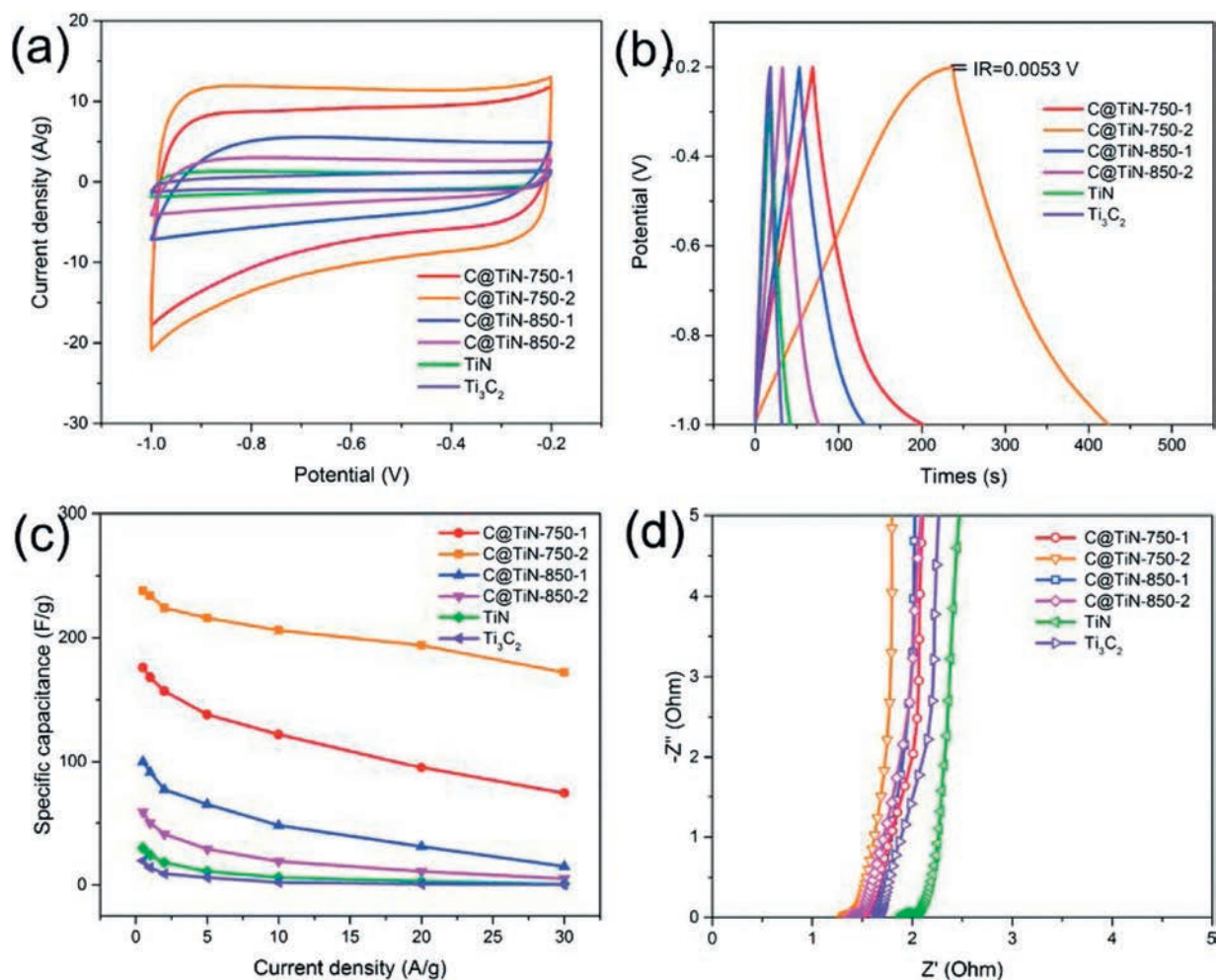


Fig. 6. (a) The cyclic voltammograms at scan of 100 mV/s. (b) Charge/discharge curve under J of 1 A/g. (c) the specific capacitance vs current density. (d) Nyquist plots of C@TiN-750-1, C@TiN-750-2, C@TiN-850-1, C@TiN-850-2, TiN and Ti₃C₂. Reproduced with permission [35]. Copyright 2018, Royal Society of Chemistry.

generated carbon atoms are deposited on the surface of TiN nanosheet. Then, the C@TiN hybrid structure was formed, as shown in (Figs. 4 and 5).

3. Hybrid nanomaterial derived from MXene for advanced energy application

3.1. Energy storage

3.1.1. Supercapacitor

An advanced electrochemical storage device is known as a supercapacitor (SC) or electrochemical capacitor. The supercapacitor has received great attraction in both academia and industry sector owing to their excellent power density, rapid charge/discharge rate, less expensive and long cycling life [36]. As seen above, ideal electrode material should have high electrical conductivity, electrochemical stability and high specific capacitance. Thus, an interesting strategy to solve these drawbacks is to use carbon/metal nitrides composites as the supercapacitor electrodes. Besides, they have significant properties like excellent electrical conductivity, high power density, energy density and provide the large specific capacitance compared to metal oxides and carbon material, respectively. Recently layered metal nitrides have more attraction in the SCs. For instance, Djire *et al.* demonstrated the nitride based MXene such as Ti_2NT_x for *pseudo* capacitance in Mg ion electrolyte [37]. Ti_2NT_x electrode shows high specific capacitance value of 200F/g at 1.0V range in Mg-ion

electrolyte. The cycle stability test exhibits the capacitance increase of 160% of its initial value even after 1000 cycles. Till date, only two nitride-based MXene electrode materials have been reported. Recently, Guo group implemented a novel route to derive metal nitrides from MXene ($\text{Ti}_3\text{C}_2\text{T}_x$), which is beneficial for supercapacitor applications. In which, the as-synthesized TiN/C-750-2 act as electrode in supercapacitor and shows specific capacitance of 238 F/g at 0.5 A/g and ultra-high cyclic stability after 10,000 cycles with high capacitance retention of 93.1% with an energy density of 5.46 Wh/kg and a power density of 111 W/kg are shown in Fig. 6 [35]. These results suggested that carbon provides fast electron transfer rate and improved cyclic stability of TiN in electrolyte. Furthermore, 2D layered carbon wrapped TMNs are expected to play a vital role in energy conversion and storage technology.

3.1.2. Lithium ion batteries (LIB)/Sodium ion batteries (SIB)

Over the decades, lithium- and sodium-ion batteries have received considerable attention as the most prominent electrochemical energy storage systems for a wide range application owing to their high coulombic efficiency, high energy densities, low cost, high stable, excellent electrical conductivities and smaller product. Although all of Ni-ion, Ca-ion, Mg-ion, K-ion and Al-ion batteries have been investigated [38–45], the development of new electrode material for LIB and SIB is essential. In this context, a class of 2D hybrids from MXene can be used to enhance the performance of lithium-ion battery. For example, Liu *et al.* developed TiO_2

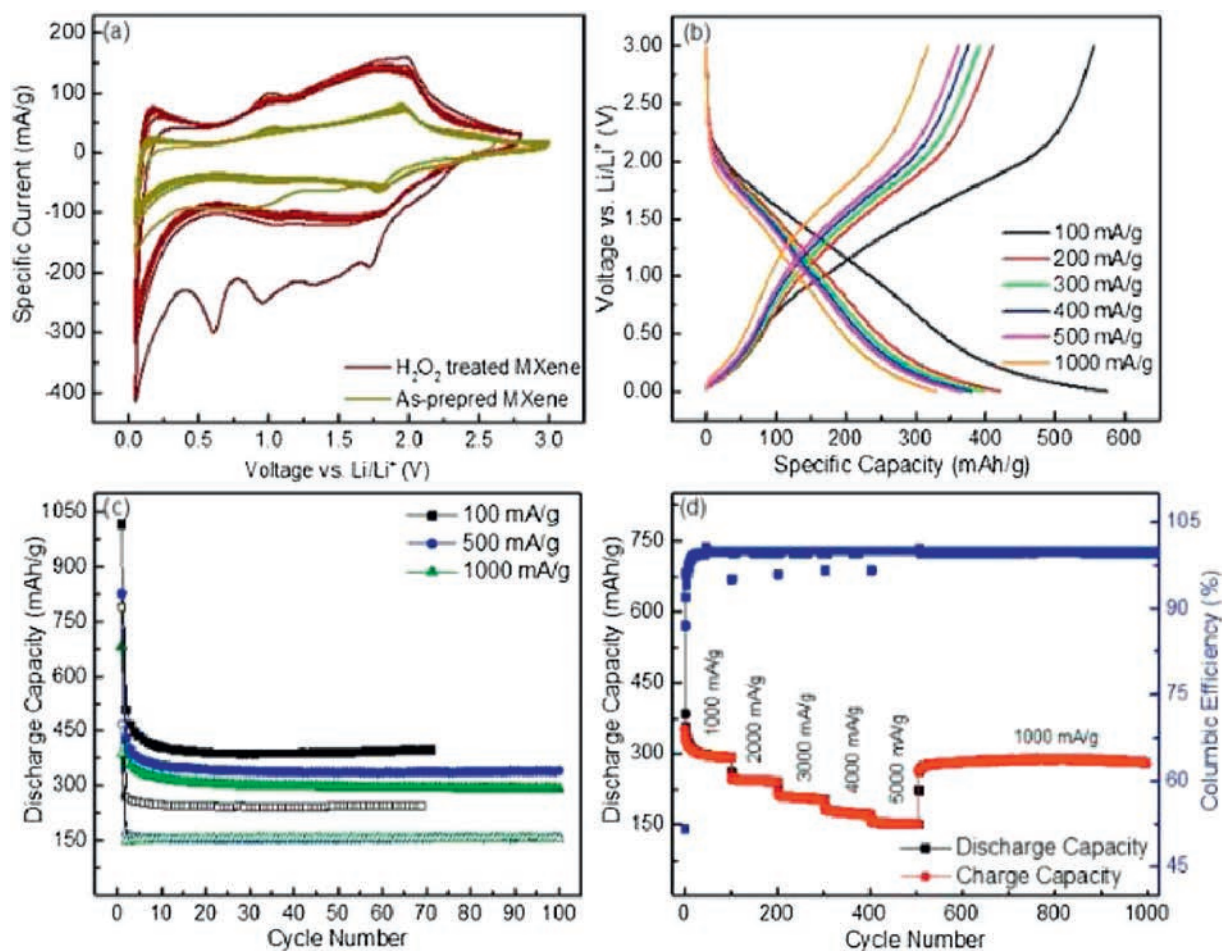


Fig. 7. (a) The cyclic voltammetry curves and (b) charge/discharge curves for the treated MXene with H_2O_2 . (c) Cyclic stability performance at 100 mA/g, 500 mA/g and 1000 mA/g. (d) Rate-ability assessment of H_2O_2 treated MXene (≈ 5 min) at various current densities. Reproduced with permission [47]. Copyright 2016, Royal Society of Chemistry.

nanostructures on MXene ($\text{Ti}_3\text{C}_2\text{T}_x$) nanosheets though van der Waals interaction for lithium ion batteries application. Addition of MXene nanosheets enhances the electrical conductivity of the electrode material and the layered structure facilitates the ion transport and prevent the aggregation of TiO_2 nano rod. As a result, $\text{TiO}_2/\text{MXene}$ heterostructures can deliver high capacity of 209 mAh/g in the voltage range 0.01–3 V at 1 C cycling rate [46]. In order to improve electrochemical performance, Ahmed *et al.* demonstrated H_2O_2 treated MXene as anode electrode material for lithium-ion batteries. This hybrid nanomaterial ($\text{TiO}_2/\text{Ti}_2\text{C}$) derived from MXene ($\text{Ti}_3\text{C}_2\text{T}_x$) can deliver a specific capacitance of 297 mAh/g at the current density of 1000–5000 mA/g. Partial oxidation MXene exhibits excellent cyclic stability of specific capacity of 280 mAh/g at the 1000th cycle (Fig. 7). In this work, the opening/swelling of MXene layers due to the treatment of H_2O_2 and titania formation cause for the large surface area accessible to Li-ions, which accounts for the improved lithium ion battery performance. Furthermore, high rate performance and outstanding cyclic stability of partially oxidized MXene are expected to be the viable candidate for Li-ion capacitors [47]. In addition, Dong *et al.* described the sodium-ion batteries using sodium titanate nanoribbons as cathode from derived Ti_3C_2 MXene. As a result, the M-NTO nanoribbons can exhibit large reversible capacity of 191 mAh/g at 200 mA/g for sodium storage, higher than those parent Ti_3C_2 (178 mAh/g) and commercial TiC derivatives (86 mAh/g) and highly long-term stability [48].

3.2. Energy conversion

Currently, water splitting process via electrochemical and photocatalytic are effective methods to produce hydrogen in large-scale with zero carbon emission [49]. These are advantageous as a sustainable energy source, but the other and main critical requirement is high-efficient catalyst. Where, 2D based nanomaterial has attractive for this particular application owing to their excellent optical, electrical properties and high surface area [50–53]. In this regard, Yuan *et al.* demonstrated that the 2D-layered carbon/ TiO_2 hybrid architecture nanomaterial derived from Ti_3C_2 , followed by the isothermal oxidation in a CO_2 atmosphere, produces relatively high photocatalytic H_2 evolution. From their optimized sample, hydrogen generation rate can reach 24.04 mmol/h for C/ TiO_2 samples, which is 89-fold higher than pure TiO_2 sample calcined at 900 °C. From photocurrent measurements, they concluded that the highest photocurrent density value of 0.024 mA/cm² is higher than pure TiO_2 (0.005 mA/cm²). This enhanced value is attributed to the higher charge separation efficiency and fast electron transfer rate in C/ TiO_2 . The apparent quantum yield (AQY) of C/ TiO_2 -700-150 at 450 nm, 420 nm and 400 nm are calculated to be 0.17%, 0.51% and 1.98%, respectively. Further, the cyclic stability of C/ TiO_2 -700-150 catalyst was tested and provides almost constant H_2 generation amount even after 8th cycle, specifying excellent cyclic stability which is shown in (Fig. 8) [54]. The hybrid nanomaterial plays a key role in improving

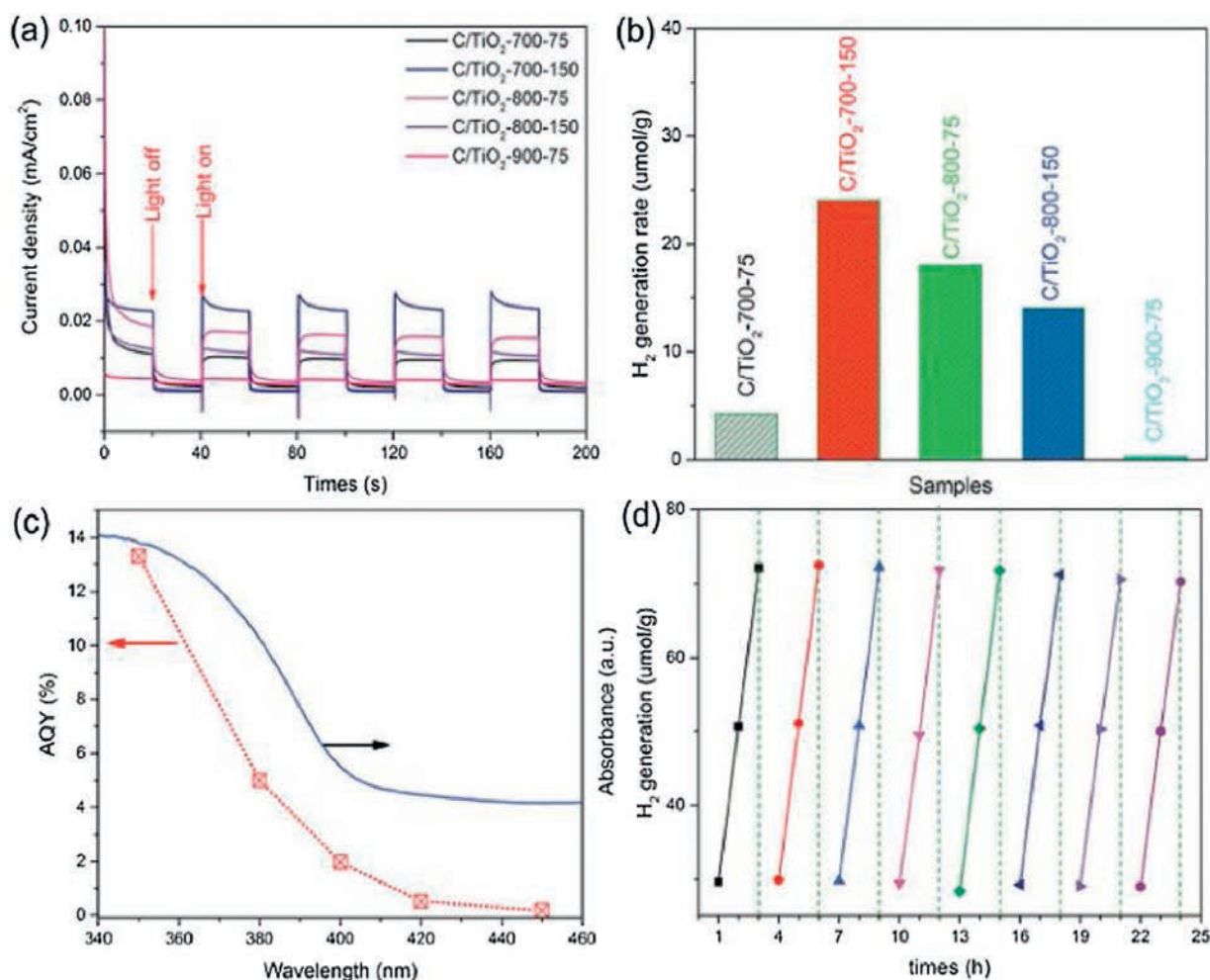


Fig. 8. (a) Transient photocurrent measurement of 2D-layered C/ TiO_2 catalyst under periodic light on/off region. (b) Comparison of hydrogen evolution rate of 2D-layered C/ TiO_2 samples. (c) AQY of C/ TiO_2 -700-150. (d) Cyclic stability of 2D-layered C/ TiO_2 -700-150. Reproduced with permission [54]. Copyright 2017, Wiley Online Library.

photocatalytic performances, the 2D carbon serves as the electron transfer conductor to enhance the charge separation of the recombination pairs. Whereas, TiO_2 nanosheets provides electron and hole *via* reducing decay of light intensity. Thus, 2D-layered C/ TiO_2 hybrids structures lead to enhanced photocatalytic H_2 generation activity. More recently, Guo *et al.* fabricated a novel laminated defect-controlled carbon supported sulfur-doped TiO_2 junction photocatalyst (LDC-S- TiO_2 /C). Further, an optimized sample of LDC-S- TiO_2 /C produced hydrogen evolution with a rate of 333 mmol/h which was much higher than that of bare rutile TiO_2 catalyst [55] as well as 27 mmol/h of C/ TiO_2 [54].

4. Prospect and outlook

In summary, this review highlights the recent advances on 2D layered MXene ($\text{Ti}_3\text{C}_2\text{T}_x$) derived hybrid nanomaterial for energy storage and conversion including supercapacitor, lithium-ion batteries, sodium-ion batteries and photo-catalytic application. In addition to, a summary of wide investigations carried out in 2D MXene has been outlined. The electrochemical performance of the MXene based hybrid nanomaterial is enhanced by high electrical conductivity, hydrophilicity, large specific surface area and stability. In spite of the numerous advantages to this material, there are still many challenges hindering their particular application. From these aspects, 2D MXene ($\text{Ti}_3\text{C}_2\text{T}_x$) derived hybrid nanomaterial have shown greater efficiency in lithium- and sodium-ion batteries, supercapacitor and water splitting applications. Generally, it was convinced that this novel hybrid nanomaterial derived from MXene has good potential in producing new alternatively energy in the future.

Declaration of competing interest

We declare that we do not have any commercial or associative interest to this work.

Acknowledgments

We thank the funding support from the Science and Technology Committee of Shannxi Province (No. 2011KGXX47), the fund of the State Key Laboratory of Solidification Processing in NWP (No. SKLSP201845) are bounded together, which hinders the oxidation process.

References

- [1] N.S. Lewis, *Science* 315 (2007) 798–801.
- [2] H.C. Tao, Y.A. Gao, N. Talreja, *et al.*, *J. Mater. Chem. A* 5 (2017) 7257–7284.
- [3] M.S. Dresselhaus, I.L. Thomas, *Nature* 414 (2001) 332.
- [4] P. Edwards, L. Kuznetsov, W. David, *et al.*, *Energy Policy* 36 (2008) 4356–4362.
- [5] O.A. Mustafa, *Renew. Sustain. Energy Rev.* 12 (2008) 2265–2300.
- [6] M.A. Rosen, D.S. Scott, *Int. J. Hydrogen Energy* 23 (1998) 653–659.
- [7] R. Ganesan, J. Lee, *J. Power Sources* 157 (2006) 217–221.
- [8] K.S. Novoselov, A.K. Geim, D. Jiang, *Science* 306 (2004) 666–669.
- [9] L. Boubekeur, H. Oughaddou, H. Enriquez, *Appl. Phys. Lett.* 97 (2010) 223109.
- [10] M.E. Davila, L. Xian, S. Cahangirov, *et al.*, *New J. Phys.* 9 (2014) 095002.
- [11] M. Topsakal, E. Aktürk, H. Şahin, *et al.*, *Phys. Rev. Lett.* 102 (2009) 236–804.
- [12] L.H. Adam, T. Neal, Z. Zhu, Z. Luo, *et al.*, *ACS Nano* 8 (2014) 4033–4041.
- [13] L. Li, Y. Yu, G. Jun Ye, *et al.*, *Nat. Nanotechnol.* 9 (2014) 372.
- [14] P. Joensen, R.F. Per, S. Frindt, Roy Morrison, *Mater. Res. Bull.* 21 (1986) 457–461.
- [15] D. Pacile, J.C. Meyer, Ç.O. Girit, *et al.*, *Appl. Phys. Lett.* 92 (2008) 133107.
- [16] M.D. James, K. Qiu, S.A. Shevlin, *et al.*, *Angew. Chem. Int. Ed.* 53 (2014) 9240–9245.
- [17] L. Yang, H. Wang, L. Xie, *et al.*, *J. Am. Chem. Soc.* 133 (2011) 7296–7299.
- [18] N. Michael, M. Kurtoglu, V. Presser, *et al.*, *Adv. Mater.* 23 (2011) 4248–4253.
- [19] N. Michael, Y. Gogotsi, *ACS Chem. Res.* 48 (2014) 128–135.
- [20] K. Narendra, B. Ahmed, Y. Gogotsi, *et al.*, *Adv. Energy Mater.* 6 (2016) 1601372.
- [21] T. Quan, M. Dahlqvist, J. Lu, *et al.*, *Nat. Commun.* 8 (2017) 14949.
- [22] N. Michael, O. Mashtalir, J. Carle, *et al.*, *ACS Nano* 6 (2012) 1322–1331.
- [23] G. Yu, L. Wang, A. Zhou, *et al.*, *Mat. Lett.* 150 (2015) 62–64.
- [24] N. Michael, M. Kurtoglu, V. Presser, *et al.*, *Adv. Mater.* 23 (2011) 4248–4253.
- [25] O. Mashtalir, M. Naguib, V.N. Mochalin, *et al.*, *Nat. Commun.* 4 (2013) 1716.
- [26] W. Zhang, W. Wei, W. Liu, *et al.*, *Chem. Eng. J.* 378 (2019) 122170.
- [27] H. Joseph, M.R. Lukatskaya, K.M. Cook, *et al.*, *Chem. Mater.* 26 (2014) 2374–2381.
- [28] S. Faisal, M. Alhabeab, C.B. Hatter, *et al.*, *Science* 353 (2016) 1137–1140.
- [29] E. Andrey, A.L. Ivanovskii, *J. Phys. Chem. C* 26 (2013) 13637–13643.
- [30] M. Cook, V.N. Mochalin, M. Crowe, *et al.*, *J. Mater. Chem. A* 2 (2014) 14334–14338.
- [31] N. Michael, O. Mashtalir, M.R. Lukatskaya, *et al.*, *Chem. Commun.* 50 (2014) 7420–7423.
- [32] H. Mei, X. Yin, X. Li, B. Anasori, *et al.*, *ACS Appl. Mater. Interfaces* 9 (2017) 20038–20045.
- [33] L. Jing, S. Wang, Y. Du, *et al.*, *Ceramics Int.* 44 (2018) 7042–7046.
- [34] A. Bilal, D.H. Anjum, M.N. Hedhili, *et al.*, *Nanoscale* 8 (2016) 7580–7587.
- [35] J. Liu, Z.X. Wang, J. Yang, *et al.*, *Mater. Lett.* 256 (2019) 126646.
- [36] W. Yuan, L. Cheng, X. Guo, *et al.*, *Chem. Commun.* 54 (2018) 2755–2758.
- [37] B. Muhammad, B. Anasori, C. Voigt, *et al.*, *Adv. Mater.* 28 (2016) 1517–1522.
- [38] D. Abdoulaye, A. Bos, J. Liu, H. Zhang, *et al.*, *ACS Appl. Nano Mater.* 2 (2019) 2785–2795.
- [39] L. Shuang, X. Cao, C.N. Schmidt, *et al.*, *J. Mater. Chem. A* 4 (2016) 4242–4251.
- [40] N. Michael, J. Come, B. Dyatkin, *et al.*, *Electrochem. Commun.* 16 (2012) 61–64.
- [41] X.Y. Dall Agnese, M. Naguib, M. Gogotsi, *et al.*, *ACS Nano* 8 (2014) 9606–9615.
- [42] A. Fadwa, A. Du Pasquier, T. Zheng, *J. Electrochemical. Soc.* 148 (2001) 930–939.
- [43] B. Lee, E. Jo, J. Choi, *et al.*, *J. Mater. Chem. A* 7 (2019) 25619–25627.
- [44] B. Goodenough, K. Park, *J. Am. Chem. Soc.* 135 (2013) 1167–1176.
- [45] P.M. Rosa, *Chem. Soc. Rev.* 38 (2009) 2565–2575.
- [46] Y.T. Liu, P. Zhang, N. Sun, *et al.*, *Adv. Mater.* 30 (2018) 170–334.
- [47] B. Ahmed, Y. Gogotsi, H.N. Alshareef, *Nano Energy* 34 (2017) 249–256.
- [48] D. Yanfeng, Z.S. Wu, S. Zheng, *et al.*, *ACS Nano* 11 (2017) 4792–4800.
- [49] W. Yuan, L. Cheng, X. Guo, *et al.*, *ACS Sus. Chem. Eng.* 6 (2018) 8976–8982.
- [50] Z. Yu, X. Xia, F. Shi, *et al.*, *Adv. Sci.* 3 (2016) 1500286.
- [51] G. Zhong, J. Zhou, L. Zhu, *et al.*, *J. Mater. Chem. A* 4 (2016) 11446–11452.
- [52] L. Yu, X. Deng, J. Tian, *et al.*, *Appl. Mater. Today* 13 (2018) 217–227.
- [53] Y. Xue, T. Wang, W. Yin, *et al.*, *Int. J. Hydrogen Energy* 44 (2019) 2704–2710.
- [54] W. Yuan, L. Cheng, X. Guo, *et al.*, *Adv. Mater. Interfaces* 4 (2017) 1700577.
- [55] W. Yuan, L. Cheng, X. Guo, *et al.*, *Adv. Sci.* 5 (2018) 1700870.